Exact Error Rate of Dual-Channel Receiver with Remote Antenna Unit Selection in Multicell Networks

Qing Wang[1,2], Ju Liu[1], Lina Zheng[1] and Hailiang Xiong[1]
[1] School of Information Science and Engineering, Shandong University
Jinan, 250100 - China
[e-mail: {juliu, zhenglina, hailiangxiong}@sdu.edu.cn]
[2] State Key Laboratory of Integrated Services Networks, Xidian University
Xi'an 710071 - China
[e-mail: qingwang.sdu@gmail.com]
*Corresponding author: Ju Liu

Received February 10, 2016; revised May 30, 2016; accepted June 17, 2016; published August 31, 2016

Abstract

The error rate performance of circularly distributed antenna system is studied over Nakagami-*m* fading channels, where a dual-channel receiver is employed for the quadrature phase shift keying signals detection. To mitigate the Co-Channel Interference (CCI) caused by the adjacent cells and to save the transmit power, this work presents remote antenna unit selection transmission based on the best channel quality and the maximized path-loss, respectively. The commonly used Gaussian and Q-function approximation method in which the CCI and the noise are assumed to be Gaussian distributed fails to depict the precise system performance according to the central limit theory. To this end, this work treats the CCI as a random variable with random variance. Since the in-phase and the quadrature components of the CCI are correlated over Nakagami-*m* fading channels, the dependency between the in-phase and the quadrature components is also considered for the error rate analysis. For the special case of Rayleigh fading in which the dependency between the in-phase and the quadrature components can be ignored, the closed-form error rate expressions are derived. Numerical results validate the accuracy of the theoretical analysis, and a comparison among different transmission schemes is also performed.

Keywords: Co-channel interference, distributed antenna system, error rate, remote antenna unit, selection transmission

This work was supported by the National Natural Science Foundation of China (61371188), the Open Fund of State Key Laboratory of Integrated Services Networks (ISN14-03), the Research Fund for the Doctoral Program of Higher Education (20130131110029), and the Natural Science Foundation of China (61401253).

1. Introduction

Multiple-antenna systems in cellular networks have garnered rising interest due to the fast growing demand for higher data rates [1-2]. Unlike the traditional Co-Located Antenna System (CAS) in which antennas are deployed around the Central Base Station (CBS), the Remote Antenna Units (RAUs) in Distributed Antenna System (DAS) are geographically deployed but connected to the CBS via optical backhaul [3]. This architecture forms a virtual cooperative network which can acquire macro-diversity gain [4]. The average distance between transmitters and recievers can be shortened, which leads to mitigating the path-loss and saving the transmit power [5-6].

However, in the multicell DAS, the performance is constrained by the Co-Channel Interference (CCI) produced from the adjacent cells [7]. The impact of the CCI on the system performance is more serious for a cell edge User Equipment (UE) [8]. To this end, various approaches to mitigate the CCI have been proposed. One effective method to alleviate the negative impact of the CCI is to employ the antenna selection scheme [9]. The authors in [10] and [11] presented a minimized bit-error rate (BER) based antenna selection scheme, and investigated the spectral efficiency with frequency reuse. The antenna selection strategies based on the RAUs cooperative transmission and the pilot signals in [12] and [13] were utilized for the system performance analysis. Li et al. proposed antenna selection algorithms based on the path-loss and energy efficiency for homogeneous and heterogeneous networks, respectively [14]. An antenna selection transmission based on the maximized Signal-to-Interference-plus-Noise Ratio (SINR) was adopted to study the ergodic capacity for DAS in the multicell environment [15]. Most of the previous literatures treat the noise and the CCI as Gaussian distributed with fixed variance. The performance evaluated from this assumption can approximately depict the real performance if the number of the CCI is sufficiently large. Nevertheless, these analytical results cannot precisely depict the performance when the number of interfering signals decreases to a single digit. Although the authors in [16] used non-central limit theory to investigate the error probability, the analytical results derived from Gaussian and Q-function cannot match the accurate performance. In addition, compared to Binary Phase Shift Keying (BPSK) signals, little work have been done on the bandwidth efficient Quadrature Phase Shift Keying (QPSK) modulation signals in multicell DAS [17]. It is noted by [18] that the Nakagami-*m* distribution can unify various fading channels with different degrees of severity, and it is a suitable model to depict the propagation of the desired signal and the CCI. Since signals experience multipath fading with different severities in DAS, Nakagami-*m* fading channel is used in this study. As the in-phase and the quadrature components of the signals are correlated over Nakagami-*m* fading channels [19], it is essential to consider the dependency between the two components of the signals for the precise performance analysis in the multicell environment.

In this paper, we study the exact error rate performance of the circularly DAS based on the RAU selection transmission. This architecture has a flexible and open infrastructure, leading to tractable performance analysis. The contributions of this paper are as follows. Unlike most previous studies in which the noise and the CCI are assumed to be Gaussian distributed, we treat the CCI as a random variable with non-constant variance. The dependency between the in-phase and the quadrature components of the CCI is considered with dual-channel reception over Nakagami-*m* fading channels. To reduce the CCI, we present two RAU selection schemes based on the Best Channel Quality (BCQ) and the Maximized Path-Loss (MPL),

respectively, and derive the theoretical error rate expressions over Nakagami-*m* fading channels. For the special case of Rayleigh fading channels, the closed-form expressions for the two selection schemes are developed. Finally, performance results are provided to verify the correctness of our derived theoretical expressions. The RAU selection transmission is also proved to bring much performance enhancement compared with the traditional DAS.

The rest of this paper is organized as follows. In Section 2, the system model is illustrated. The precise error-rate performance of DAS in the multicell environment is derived in Section 3. The numerical and simulation results are presented in Section 4. Finally, the conclusions are provided in Section 5.

2. System Model

In this paper, we study the circularly DAS with $N+1$ cells. The CBS located at each cell center has the ability of a RAU and the Base Station Controller (BSC). The other k RAUs are uniformly deployed across a circle with radius r $(0<r<R)$, where R denotes the radiation radius of each cell. In this architecture, $k+1$ RAUs are geographically deployed in a cell, but they are connected to the CBS via optical backhaul, as shown in **Fig. 1**. According to the geometrical relationship, the angles between any two adjacent RAUs is $2\pi/k$. Therefore, this architecture equals to one-dimentional network. The macro-diversity gain can be obtained with such virtual cooperative networks formed by $L=k+1$ RAUs. Without loss of generality, all the RAUs and the UEs are assumed to be equipped with an omnidirectional antenna.

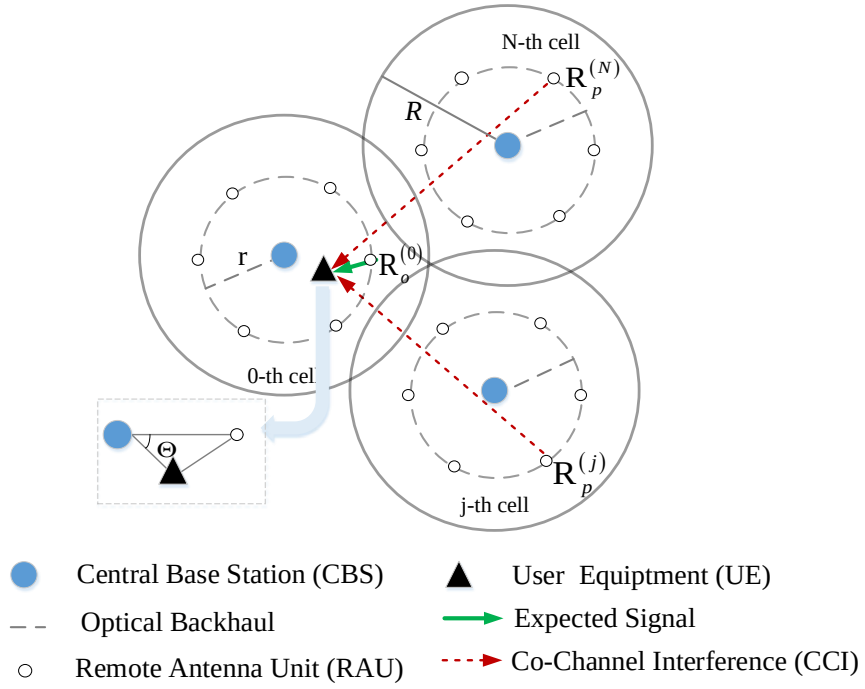

Fig. 1. Circularly distributed antenna system model

Among all the cells, the target cell is denoted as the 0-th cell, and the remaining cells are defined as the adjacent cells. The i th RAU in the j th cell is denoted as $R_i^{(j)}$, where

$i \in \{0,1,...,k\}$ and $j \in \{0,1,...N\}$. Let $P_i^{(j)}$ be the transmit power of $\mathrm{R}_i^{(j)}$, then the total transmit power of a cell is $P^{(j)} = \sum_{i=0}^{k} P_i^{(j)}$. It is assumed that in a time block, only one UE is served under the Time Division Multiple Access (TDMA) protocol. All the bandwidth efficient QPSK modulation signals experience frequency non-selective fading, and the dual-channel receiver can acquire the channel state information.

In the multicell DAS, the UE may communicate with one or more RAUs simultaneously, depending on its location and the channel conditions. In order to mitigate the CCI, as well as to save the transmit power, we exploit the RAU selection transmission. Inspired by W. Choi and I. G. Andrews [9], a RAU denoted by $\mathrm{R}_o^{(0)}$ is selected to serve the UE in the target cell, as shown in **Fig. 1**. Whereas in each adjacent cells, one RAU indexed by p is slected to transmit interfering signal to the UE. Compared to the traditional DAS in which all the RAUs are employed for transmission, RAU selection transmission can greatly reduce the number of CCI. The transmit signals from the target cell and the j th adjacent cells can be expressed respectively, as:

$$X_o(t) = \sqrt{P_o^{(0)}T}\, s_{oi}^{(0)}(t)\sin\omega_c t + \sqrt{P_o^{(0)}T}\, s_{oq}^{(0)}(t)\cos\omega_c t \tag{1}$$

and

$$X_p^{(j)}(t) = \sqrt{P_p^{(j)}T}\, s_{pi}^{(j)}(t)\sin\omega_c t + \sqrt{P_p^{(j)}T}\, s_{pq}^{(j)}(t)\cos\omega_c t \tag{2}$$

where ω_c denotes the carrier frequency, and $1/T$ is the symbol rate. $s_{oi}^{(0)}(t)$ and $s_{oq}^{(0)}(t)$ denote the in-phase and the quadrature components of the expected baseband signal; $s_{pi}^{(j)}(t)$ and $s_{pq}^{(j)}(t)$ represent the in-phase and the quadrature components of the interfering baseband signal from the j th cell. They are given by

$$\begin{cases} s_{oi}^{(0)}(t) = \sum\limits_{k=-\infty}^{+\infty} a_{oi}^{(0)}[k]\, c_T(t_0) \\ s_{oq}^{(0)}(t) = \sum\limits_{k=-\infty}^{+\infty} a_{oq}^{(0)}[k]\, c_T(t_0) \\ s_{pi}^{(j)}(t) = \sum\limits_{k=-\infty}^{+\infty} b_{pi}^{(j)}[k]\, c_T(t_j) \\ s_{pq}^{(j)}(t) = \sum\limits_{k=-\infty}^{+\infty} b_{pq}^{(j)}[k]\, c_T(t_j) \end{cases} \tag{3}$$

where $t_0 = t - kT$, $t_j = t - kT - \tau_j$, τ_j is the symbol timing offset between the desired signal and the j th interfering signal which is uniformly distributed in $[0,T]$. $a_{oi}^{(0)}[k]$, $a_{oq}^{(0)}[k]$, $b_{pi}^{(j)}[k]$, and $b_{pq}^{(j)}[k]$ denote the information bits taking values of +1 or −1 with equal probability, and c_T is the pulse forming formula with unit power.

Let $h_i^{(j)} \sim \text{Nakagami}\left(\Omega_i^{(j)}, m_i^{(j)}\right)$ be the small-scale random variable, where $\Omega_i^{(j)} = \mathbf{E}\left\{\left|h_i^{(j)}\right|\right\}^2$ ($\mathbf{E}\{\cdot\}$ denotes the expectation operation), and the fading parameter, $m_i^{(j)}$, takes values from $\left[1/2, \infty\right)$. The path-loss, $L_i^{(j)}$, can be calculated as $L_i^{(j)} = \left(d_i^{(j)}\right)^{-\alpha}$, where α is the path-loss exponent and $d_i^{(j)}$ represents the distance between the UE and $\mathrm{R}_i^{(j)}$. Then, the channel coefficient can be written as $g_i^{(j)} = h_i^{(j)}\sqrt{L_i^{(j)}}$. Since the in-phase channel and the quadrature channel have symmetry, without loss of generality, we analyze the performance via the in-phase channel detection for the expected signal. It is assumed that the expected signals and CCI have the same symbol timing in the multicell DAS. After demodulation, matched filtering, and completing carrier recovery, during a given time block, the decision statistic is expressed as

$$\begin{aligned} r_0 = &\sqrt{P_o^{(0)}T}\, g_o^{(0)} a_{oi}^{(0)}[0] + \sum_{j=1}^{N}\left\{\sqrt{P_p^{(j)}T}\, g_p^{(j)} \sin\left(\phi_p^{(j)}\right) b_{pi}^{(j)}[0]\right. \\ &\left. + \sqrt{P_p^{(j)}T}\, g_p^{(j)} \cos\left(\phi_p^{(j)}\right) b_{pq}^{(j)}[0]\right\} + n_0 \end{aligned} \tag{4}$$

where $\phi_p^{(j)}$ is the random phase difference produced by demodulation which is uniformly distributed in $\left[0, 2\pi\right)$, and n_0 is the additive Gaussian noise. It is observed from equation (4) that the system performance is related to the expected signal, the in-phase component of the CCI, and the quadrature component of the CCI.

3. Error Rate Performance of DAS

A common approach for analyzing the DAS performance is the Gaussian and Q-Function Approximation (GQA), i.e., the CCI and the noise at the receiver are treated as a Gaussian variable with fixed variance. According to the central limit theory, the accuracy of the performance estimated degrades as the number of the interfering signals decreases. Since the number of the interfering signals is reduced by adopting the RAU selection transmission based on the BCQ and the MPL, for precise error rate analysis, we treat the CCI as the random variable with random variance and consider the dependency between the in-phase and the quadrature components of the CCI. As mentioned previously, the receiver with dual-channel reception detects the in-phase and the quadrature components of the QPSK signal separately. In general, these two components are correlated over Nakagami-*m* fading channels. As a consequence, apart from the channel power fading gain, the dependency between the components of the CCI should be considered.

Let $\beta_i^{(0)} = P_i^{(0)}T\left|g_i^{(0)}\right|^2$, and $\chi_i^{(0)} = m_i^{(0)} / P_i^{(0)}TL_i^{(0)}\Omega_i^{(0)}$. Since the small-scale fading parameter, $h_i^{(0)}$, follows Nakagami-*m* distribution, the Cumulative Distribution Function (CDF) can be expressed as ($m_i^{(0)}$ is an integer)

$$\begin{aligned} F_{\beta_i^{(0)}}(\beta) &= \Gamma\left(m_i^{(0)}\right)\Upsilon\left(m_i^{(0)}, \chi_i^{(0)}\beta\right) \\ &= 1-\exp\left(-\chi_i^{(0)}\beta\right)\sum_{n=0}^{m_i^{(0)}-1}\frac{\left(\chi_i^{(0)}\beta\right)^n}{\Gamma(n+1)} \end{aligned} \tag{5}$$

where $\Upsilon(\cdot,\cdot)$ represents the incomplete Gamma function [20]. We denote $\Delta = I + n_0$, where I is the totol CCI which can be given by

$$I = \sum_{j=1}^{N}\left\{\sqrt{P_p^{(j)}T}\,g_p^{(j)}\sin\left(\phi_p^{(j)}\right)b_{pi}^{(j)}[0] + \sqrt{P_p^{(j)}T}\,g_p^{(j)}\cos\left(\phi_p^{(j)}\right)b_{pq}^{(j)}[0]\right\} \tag{6}$$

Since β_o denotes the channel gain between $\mathrm{R}_o^{(0)}$ and the UE, the conditional error rate of the in-phase component of the expected QPSK signal can be obtained as

$$\begin{aligned} P_{e|\beta_o=\beta} &= \Pr\left\{\sqrt{\beta_o}a_{oi}[0] + \Delta < 0 \middle| \beta_o = \beta, a_{oi}[0] = +1\right\} \\ &= 1 - F_\Delta\left(\sqrt{\beta}\right) \\ &= \frac{1}{2} - \frac{1}{\pi}\int_0^\infty \frac{1}{\omega}\sin\left(\sqrt{\beta}\omega\right)M_\Delta(\omega)\,\mathrm{d}\omega \end{aligned} \tag{7}$$

where $M_\Delta(\omega)$ is the characterisitic function of the CCI plus noise. Therefore, it is essential to analyze $M_\Delta(\omega)$. In this section, we assume $\overline{G}_p^{(j)} = g_p^{(j)}\sin\left(\phi_p^{(j)}\right)$ and $\overline{\overline{G}}_p^{(j)} = g_p^{(j)}\cos\left(\phi_p^{(j)}\right)$ denote the in-phase and the quadrature contributions of the CCI from the j th cell, respectively. The CCI of the j th cell can be written as

$$I_p^{(j)} = \sqrt{P_p^{(j)}T}\,\overline{G}_p^{(j)}b_{pi}^{(j)}[0] + \sqrt{P_p^{(j)}T}\,\overline{\overline{G}}_p^{(j)}b_{pq}^{(j)}[0] \tag{8}$$

Then, the conditional characteristic function of the CCI is obtained as

$$\begin{aligned} M_{I_p^{(j)}\left|\bar{h}_j,\bar{\bar{h}}_j\right.}(\omega) &= \mathrm{E}\left\{e^{i\omega I_p^{(j)}\left|\bar{h}_j,\bar{\bar{h}}_j\right.}\right\} \\ &= \cos\left(\sqrt{P_p^{(j)}L_p^{(j)}T}\,\bar{h}_j\omega\right)\cos\left(\sqrt{P_p^{(j)}L_p^{(j)}T}\,\bar{\bar{h}}_j\omega\right) \end{aligned} \tag{9}$$

In this place, the joint Probability Density Function (PDF) of the random variables $\overline{H}_p^{(j)} = h_p^{(j)}\sin\left(\phi_p^{(j)}\right)$ and $\overline{\overline{H}}_p^{(j)} = h_p^{(j)}\cos\left(\phi_p^{(j)}\right)$ are derived from [19] as

$$f_{\overline{H}_p^{(j)},\overline{\overline{H}}_p^{(j)}}\left(\bar{h}_j,\bar{\bar{h}}_j\right) = \frac{m_p^{(j)m_p^{(j)}}}{\pi\left(\Omega_p^{(j)}\right)^{m_p^{(j)}}\Gamma\left(m_p^{(j)}\right)}\left(\bar{h}_j^2+\bar{\bar{h}}_j^2\right)^{m_p^{(j)}-1}e^{-\frac{m_p^{(j)}\left(\bar{h}_j^2+\bar{\bar{h}}_j^2\right)}{\Omega_p^{(j)}}} \tag{10}$$

Averaging over the PDF of $\overline{H}_p^{(j)}$ and $\overline{\overline{H}}_p^{(j)}$, one obtains the characteristic function of the total CCI as

$$M_I(\omega)=\prod_{j=1}^{N}\frac{4m_p^{(j)m_p^{(j)}}}{\pi\left(\Omega_p^{(j)}\right)^{m_p^{(j)}}\Gamma\left(m_p^{(j)}\right)}\int_0^\infty\int_0^\infty\left(\bar{h}_j^2+\bar{\bar{h}}_j^2\right)^{m_p^{(j)}-1}e^{-\frac{m_p^{(j)}\left(\bar{h}_j^2+\bar{\bar{h}}_j^2\right)}{\Omega_p^{(j)}}}$$
$$\times\cos\left(\sqrt{P_p^{(j)}L_p^{(j)}T}\,\bar{h}_j\omega\right)\cos\left(\sqrt{P_p^{(j)}L_p^{(j)}T}\,\bar{\bar{h}}_j\omega\right)\mathrm{d}\,\bar{h}_j\,\mathrm{d}\,\bar{\bar{h}}_j \tag{11}$$

As the CCI and the noise are uncorrelated, the term $M_\Delta(\omega)$ can be rewritten as $M_\Delta(\omega)=M_I(\omega)M_{n_0}(\omega)$. Since the characteristic function of the noise is given by $M_{n_0}(\omega)=\exp\left(-\omega^2/2\right)$, the exact $M_\Delta(\omega)$ can be derived. Applying $M_\Delta(\omega)$ into equation (7) and averaging over the PDF of β_o, we can obtain the exact error rate expression as

$$P_e=\underbrace{\int_0^\infty Q\left(\sqrt{\beta}\right)f_{\beta_o}(\beta)\mathrm{d}\beta}_{\varepsilon_1}$$
$$+\underbrace{\frac{1}{\pi}\int_0^\infty\int_0^\infty\frac{1}{\omega}\sin\left(\sqrt{\beta}\omega\right)e^{-\frac{\omega^2}{2}}\left(1-M_I(\omega)\right)f_{\beta_o}(\beta)\mathrm{d}\beta\,\mathrm{d}\omega}_{\varepsilon_2} \tag{12}$$

where both the error probabilities ε_1 and ε_2 depend on $f_{\beta_o}(\beta)$. ε_2 is also related to the characteristic function of the CCI. Using Fourier Inversion, the PDF of the in-phase contribution of the CCI can be calculated as

$$f_{\bar{H}_p^{(j)}}\left(\bar{h}_j\right)=\frac{1}{2\pi}\int_0^\infty e^{-i\omega h_p^{(j)}\sin\left(\phi_p^{(j)}\right)}\left[M_{\bar{H}_p^{(j)}}(\omega)\right]\mathrm{d}\omega$$
$$=\frac{\left|\bar{h}_j\right|^{2m_p^{(j)}-1}}{\sqrt{\pi}\Gamma\left(m_p^{(j)}\right)}\left(\frac{m_p^{(j)}}{\Omega_p^{(j)}}\right)^{m_p^{(j)}}e^{-\frac{m_p^{(j)}\bar{h}_j^2}{\Omega_p^{(j)}}}{}_1F_1\left(\frac{1}{2};m_p^{(j)}+\frac{1}{2};\frac{m_p^{(j)}\bar{h}_j^2}{\Omega_p^{(j)}}\right) \tag{13}$$

where $M_{\bar{H}_p^{(j)}}(\omega)=\int_0^\infty f_{h_p^{(j)}}(h)\mathrm{d}h\int_0^{2\pi}\frac{1}{2\pi}e^{ih\sin\phi\omega}\mathrm{d}\phi$, and ${}_1F_1(\cdot;\cdot;\cdot)$ denotes the confluent hypergeometric function [20]. From equations (10) and (13), we can conclude that when $m_p^{(j)}\neq 1$, $f_{\bar{H}_p^{(j)},\bar{\bar{H}}_p^{(j)}}\left(\bar{h}_j,\bar{\bar{h}}_j\right)\neq f_{\bar{H}_p^{(j)}}\left(\bar{h}_j\right)\cdot f_{\bar{\bar{H}}_p^{(j)}}\left(\bar{\bar{h}}_j\right)$, which also means the in-phase and the quadrature components of the CCI are correlated.

3.1 Best Channel Quality Based Selection Transmission

To alleviate the negative impact of the CCI, we adopt RAU selection transmission. According to equation (12), it is critical to analyze the PDF of β_o. Since $\beta_o=P_o^{(0)}TL_o^{(0)}\left|h_o^{(0)}\right|^2$, the small-scale fading, $h_o^{(0)}$, and the path-loss, $L_o^{(0)}$, are only related to the expected signal instead of the CCI. Given the specific location of the UE, the selected RAU can be chosen via the following norm:

$$G_o = \max_{i\in\{0,\ldots,k+1\}} \left\{ \left| h_i^{(0)} \right|^2 L_i^{(0)} \right\} \tag{14}$$

Let $\beta_o = P_o^{(0)} T G_o$, the CDF of β_o can be expressed as $F_{\beta_o}(\beta) = \prod_{i=1}^{k+1} F_{\beta_i^{(0)}}(\beta)$. Applying equation (5) and taking differentiation, one obtains the PDF of β_o based on the BCQ as

$$\begin{aligned} f_{\beta_o}(\beta) = & \sum_{i=1}^{k+1} (-1)^{i+1} \mathrm{Z}_1 \left(\sum_{m=1}^{i} \chi_{nm}^{(0)} \right) \exp\left(-\sum_{m=1}^{i} \chi_{nm}^{(0)} \beta \right) \mathrm{Z}_2 \left(\prod_{m=1}^{i} \frac{\left(\chi_{nm}^{(0)}\right)^{\lambda_m}}{\Gamma(\lambda_m+1)} \right) \beta^{\sum_{m=1}^{i}\lambda_m} \\ & - \sum_{i=1}^{k+1} (-1)^{i+1} \mathrm{Z}_1 \exp\left(-\sum_{m=1}^{i} \chi_{nm}^{(0)} \beta \right) \mathrm{Z}_2 \left(\prod_{m=1}^{i} \frac{\left(\chi_{nm}^{(0)}\right)^{\lambda_m}}{\Gamma(\lambda_m+1)} \right) \left(\sum_{m=1}^{i} \lambda_m \right) \beta^{-1+\sum_{m=1}^{i}\lambda_m} \end{aligned} \tag{15}$$

where the terms Z_1 and Z_2 in equation (15) are expressed as

$$\begin{cases} \mathrm{Z}_1 = \sum\limits_{n_1=1}^{k-i+2} \sum\limits_{n_2=n_1+1}^{k-i+3} \cdots \sum\limits_{n_i=n_{i-1}+1}^{k+1} \\ \mathrm{Z}_2 = \sum\limits_{\lambda_1=0}^{m_{n_1}^{(0)}-1} \cdots \sum\limits_{\lambda_i=0}^{m_{n_i}^{(0)}-1} \end{cases} \tag{16}$$

Since the error probability ε_1 only depends on $f_{\beta_o}(\beta)$, substituting equation (15) into equation (12), one obtains ε_1 as

$$\varepsilon_1 = \sum_{i=1}^{k+1} (-1)^{i+1} \mathrm{Z}_1 \left\{ \left(\sum_{m=1}^{i} \chi_{nm}^{(0)} \right) \mathrm{A}_1 - \left(\sum_{m=1}^{i} \lambda_m \right) \mathrm{A}_2 \right\} \tag{17}$$

where

$$\mathrm{A}_1 = \frac{1}{\sqrt{2\pi}} \int_0^{\infty} \int_{\sqrt{2\gamma}}^{\infty} \exp\left(-\frac{t^2}{2} - \sum_{m=1}^{i} \chi_{nm}^{(0)} \beta \right) \mathrm{Z}_2 \beta^{\sum_{m=1}^{i}\lambda_m} \left(\prod_{m=1}^{i} \frac{\left(\chi_{nm}^{(0)}\right)^{\lambda_m}}{\Gamma(\lambda_m+1)} \right) \mathrm{d}t\, \mathrm{d}\beta \tag{18}$$

and

$$\mathrm{A}_2 = \frac{1}{\sqrt{2\pi}} \int_0^{\infty} \int_{\sqrt{2\gamma}}^{\infty} \exp\left(-\frac{t^2}{2} - \sum_{m=1}^{i} \chi_{nm}^{(0)} \beta \right) \mathrm{Z}_2 \beta^{-1+\sum_{m=1}^{i}\lambda_m} \left(\prod_{m=1}^{i} \frac{\left(\chi_{nm}^{(0)}\right)^{\lambda_m}}{\Gamma(\lambda_m+1)} \right) \mathrm{d}t\, \mathrm{d}\beta \tag{19}$$

According to [21], we have

$$Q\sqrt{\beta} = \frac{1}{2} - \sqrt{\frac{\beta}{2\pi}}\, {}_1F_1\left(\frac{1}{2}; \frac{3}{2}; -\beta \right) \tag{20}$$

Applying equation (20), one calculates the closed-form ε_1 as

$$\varepsilon_1 = \frac{1}{\sqrt{2\pi}} \sum_{i=1}^{k+1} (-1)^{i+1} Z_1 Z_2 \left(\prod_{m=1}^{i} \frac{\left(\chi_{nm}^{(0)}\right)^{\lambda_m}}{\Gamma(\lambda_m + 1)} \right) \left(\sum_{m=1}^{i} \chi_{nm}^{(0)} \right)^{-\left(\frac{1}{2} + \sum_{m=1}^{i} \lambda_m\right)} (\mathrm{K}_1 - \mathrm{K}_2) \tag{21}$$

where

$$\mathrm{K}_1 = \left(\sum_{m=1}^{i} \lambda_m \right) \Gamma\left(\frac{1}{2} + \sum_{m=1}^{i} \lambda_m \right) {}_2F_1\left(\frac{1}{2}, \frac{1}{2} + \sum_{m=1}^{i} \lambda_m; \frac{3}{2}; -\frac{1}{2\sum_{m=1}^{i} \chi_{nm}^{(0)}} \right) \tag{22}$$

and

$$\mathrm{K}_2 = \Gamma\left(\frac{3}{2} + \sum_{m=1}^{i} \lambda_m \right) {}_2F_1\left(\frac{1}{2}, \frac{3}{2} + \sum_{m=1}^{i} \lambda_m; \frac{3}{2}; -\frac{1}{2\sum_{m=1}^{i} \chi_{nm}^{(0)}} \right) \tag{23}$$

As discussed previously, the error probability ε_2 depends on $f_{\beta_o}(\beta)$ and the characteristic function of the CCI simultaneously. Substituting equations (11), (15) and (21) into equation (12), one obtains the precise error rate for the circularly DAS based on the BCQ selection as:

$$P_e = \varepsilon_1 + \frac{1}{\pi} \sum_{i=1}^{k+1} (-1)^{i+1} Z_1 \int_0^{\infty} \int_0^{\infty} \frac{1}{\omega} \sin\left(\sqrt{\beta}\omega\right) e^{-\frac{s^2}{2}} \left(1 - M_I(s)\right) f_{\beta_o}(\beta) \, \mathrm{d}\beta \, \mathrm{d}\omega \tag{24}$$

It is observed from equation (24) that the error rate performance is related to the channel power fading gain of the CCI, whereas the error rate performance is not correlated with variation of the CCI if using the GQA approach.

Without loss of generality, we assume all the interfering signals experience the same fading severity, i.e., $m_p^{(j)} = m_p$, the characteristic function of $M_I(\omega)$ shown in equation (11) can be approximated by ignoring the dependency between the in-phase and the quadrature components of the CCI as

$$M_I(\omega) \approx \prod_{j=1}^{N} \left[{}_1F_1\left(m_p; 1; -\frac{\Omega_p^{(j)} L_p^{(j)} P_p^{(j)} T}{4m_p} \omega^2 \right) \right]^2 \tag{25}$$

Applying equation (25) to equation (24), we can derive the approximated error probability for the DAS with relatively low computational complexity.

Special case: When all the signals experience Rayleigh fading channels, i.e., $m_p = m_o^{(0)} = 1$, both the in-phase and the quadrature components of the CCI are independent. Then, the exact $M_I(\omega)$ shown in equation (11) can be further simplified as

$$M_I(\omega) = \exp\left(-\frac{T \sum_{j=1}^{N} \Omega_p^{(j)} L_p^{(j)} P_p^{(j)}}{2} \omega^2 \right) \tag{26}$$

Applying equation (26) to equation (24), and assuming $\nu_p = 2 + 2\Omega_p^{(j)} T \sum_{j=1}^{N} L_p^{(j)} P_p^{(j)}$, one derives the closed-form error rate expression for the DAS as

$$P_{e,R}=\frac{1}{\pi}\Gamma\left(\frac{1}{2}\right)\sum_{i=1}^{k+1}(-1)^{i+1}\mathrm{Z}_1\left(\prod_{m=1}^{i}\frac{\left(\chi_{nm}^{(0)}\right)^{\lambda_m}}{\Gamma\left(\lambda_m+1\right)}\right)\left\{\Gamma\left(i+\frac{3}{2}\right)\mathrm{O}_1-i\Gamma\left(i+\frac{1}{2}\right)\mathrm{O}_2\right\}$$
$$-\frac{1}{\sqrt{2\pi}}\Gamma\left(\frac{3}{2}\right)\sum_{i=1}^{k+1}(-1)^{i+1}\mathrm{Z}_1\sqrt{\sum_{m=1}^{i}\chi_{nm}^{(0)}}\,{}_2F_1\left(\frac{1}{2},\frac{3}{2};\frac{3}{2};-\frac{1}{2\sum_{m=1}^{i}\chi_{nm}^{(0)}}\right) \tag{27}$$

where

$$\mathrm{O}_1=\frac{1}{\sqrt{2}}\,{}_2F_1\left(i+\frac{3}{2},\frac{1}{2};\frac{3}{2};-\frac{1}{2\sum_{m=1}^{i}\chi_{nm}^{(0)}}\right)-\sqrt{\frac{1}{\nu_p}}\,{}_2F_1\left(i+\frac{3}{2},\frac{1}{2};\frac{3}{2};-\frac{1}{2\sum_{m=1}^{i}\chi_{nm}^{(0)}\nu_p}\right) \tag{28}$$

and

$$\mathrm{O}_2=\frac{1}{\sqrt{2}}\,{}_2F_1\left(i+\frac{1}{2},\frac{1}{2};\frac{3}{2};-\frac{1}{2\sum_{m=1}^{i}\chi_{nm}^{(0)}}\right)-\sqrt{\frac{1}{\nu_p}}\,{}_2F_1\left(i+\frac{1}{2},\frac{1}{2};\frac{3}{2};-\frac{1}{\sum_{m=1}^{i}\chi_{nm}^{(0)}\nu_p}\right) \tag{29}$$

3.2 Maximized Path-loss Based Selection Transmission

In this subsection, we consider the MPL based RAU selection transmission, and derive the theoretical error rate expressions for DAS in the multicell environment. In the MPL based RAU selection scheme, the RAU with the shortest distance among all the transmission links in the target cell is selected, i.e., $o=\arg\max_{i\in\{0,1,\ldots,k\}}\left\{L_i^{(0)}\right\}$. It is followed by equation (7) that

$$P_{e|\beta_o=\beta}=\frac{1}{2}-\frac{1}{\pi}\int_0^\infty\frac{1}{\omega}\sin\left(\sqrt{P_o^{(0)}L_oT}h_o^{(0)}\omega\right)M_\Delta(\omega)\mathrm{d}\omega \tag{30}$$

Since $h_o^{(0)}$ is Nakagami-*m* distributed, averaging over the PDF of $h_o^{(0)}$, one obtains the precise error rate expression for the MPL based RAU selection transmission as

$$P_e=-\sqrt{\frac{P_o^{(0)}L_o\Omega_o^{(0)}T}{m_o^{(0)}}}\frac{\Gamma\left(m_o^{(0)}+1/2\right)}{\pi\Gamma\left(m_o^{(0)}\right)}\int_0^\infty e^{-\frac{\omega^2}{2}}$$
$$\times\,{}_1F_1\left(m_o^{(0)}+\frac{1}{2};\frac{3}{2};\frac{-P_o^{(0)}L_o\Omega_o^{(0)}T\omega^2}{4m_o^{(0)}}\right)M_I(\omega)\mathrm{d}\omega \tag{31}$$

Numerical integration can be applied for the evaluation of the precise error rate with equation (11) into equation (26). Similarly, for the special case of Rayleigh fading, i.e., $m_p=m_o^{(0)}=1$, the dependency between the in-phase and the quadrature components of the CCI can be ignored. The closed-form error rate expression with Rayleigh distribution is given by

$$P_{e,R} = \frac{1}{2} - \frac{\sqrt{\kappa}}{\pi}\Gamma\left(\frac{1}{2}\right)\Gamma\left(\frac{3}{2}\right)_2 F_1\left(\frac{3}{2},\frac{1}{2};\frac{3}{2};-\kappa\right) \tag{32}$$

where $\kappa = P_o^{(0)} L_o \Omega P_o^{(0)} T / 2\left(T\sum_{j=1}^{N} \Omega_p^{(j)} L_p^{(j)} P_p^{(j)} + 1\right)$.

Compared with the error rate performance evaluated from the commonly used GQA method which is only dependent on the expected signal, the derived error rate expressions shown in equations (24), (27), (31), and (32) are also related to the power distribution of the CCI. Besides, equation (24) and equation (31) include the correlation between the in-phase and the quadrature components of the CCI.

4. Numerical Results and Analysis

In this section, simulation and numerical results are given to verify the accuracy of the theoretical results. The error-rate performance of different transmission schemes is also provided over Nakagami-*m* fading channels. In addition, the impacts of various parameters on the system performance are shown for the performance prediction. In this work, if not stated otherwise, the parameters for DAS in the multicell environment are set as follows: the number of the adjacent cells is $N = 7$, the number of RAUs in a cell is $L = k + 1$, the total transmit power of a cell is $P_t = 2\,\mathrm{dB}$, the transmit power for each RAU is P_t / L according to the equal power allocation, the radius of the circle for RAUs' deployment is $r = 0.6$, the normalized radiation radius for a cell is $R = 1.0$, the path-loss exponent is $\alpha = 4.0$, the fading severities of all the CCI are set to be the same, i.e., $m_I = m_i^{(j)}$, and the angle between the direction of the UE to the cell-central and the horizontal direction is $\Theta = \pi / 10$, as shown in **Fig. 1**.

Fig. 2 and **Fig. 3** show the error rate performance in the multicell environment based on the BCQ and the MPL, respectively. QPSK modulation signals experience Nakagami-*m* fading channels ($m_I = m_o^{(0)} = 2$) and Rayleigh fading channels, respectively. Compared with the Monte Carlo simulation results, we can conclude that the commonly used GQA approach cannot precisely predict the system performance. From **Fig. 2(a)** and **Fig. 3(a)**, which are performed over Nakagami-*m* fading channels, it is observed that the theoretical results match the Monte Carlo simulation results if the dependency between the in-phase and the quadrature components of the CCI is considered. For instance, compared with GQA, almost 54% of performance prediction can be improved with our proposed analytical method based on the BCQ selection scheme, as shown in **Fig. 2(a)**. However, the exact error rate cannot be obtained without considering the dependency between the in-phase and the quadrature components of the CCI. In the circumstance of Rayleigh fading channels, precise error rate performance can be achieved if the dependency between the two components of the CCI is ignored, as shown in **Fig. 2(b)** and **Fig. 3(b)**. Another interesting find is that the error rate performance can be improved when the UE is located at $d = 0.6$. We define this position as the improved point. This is explained by the fact that when the UE moves to this position, a RAU deployed nearby dominates the system performance.

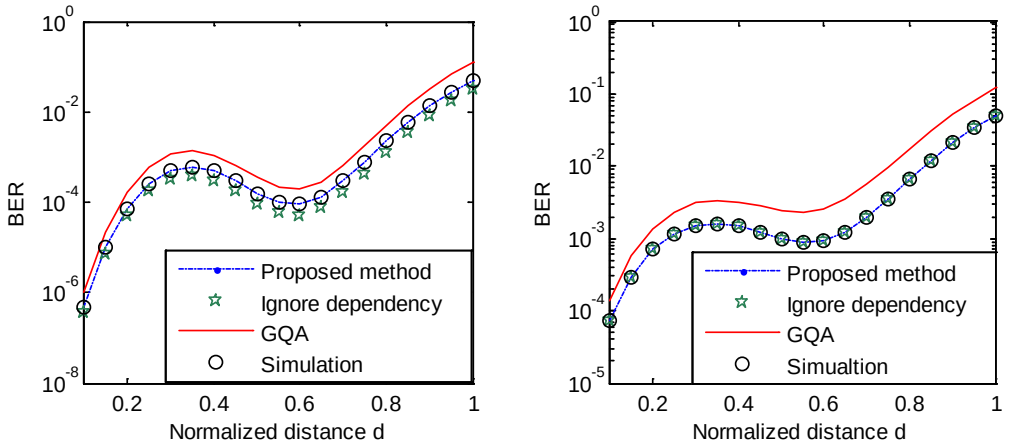

(a) Nakagami-*m* fading channels (b) Rayleigh fading channels

Fig. 2. The error rate with RAU selection based on the BCQ versus normalized distance

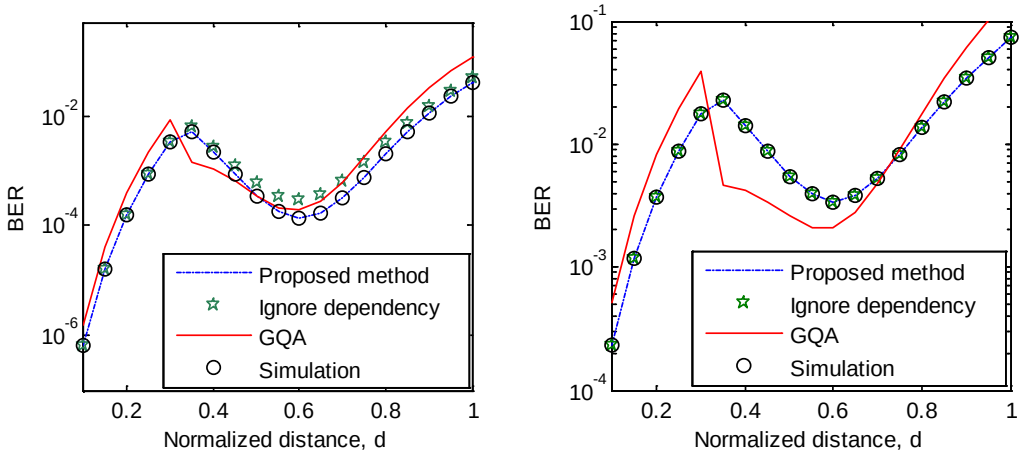

(a) Nakagami-m fading channels (b) Rayleigh fading channels

Fig. 3. The error rate with RAU selection based on the MPL versus normalized distance

Different transmission schemes are compared in **Fig. 4** when the number of the RAUs in a cell is set to be 6, and $m_I = m_o^{(0)} = 1$. The error rate obtained by the commonly used GQA method is not coincident with the precise BER, as expected. It is further observed form **Fig. 4** that in general, compared with the traditional DAS in which all the RAUs are used for transmission, the RAU selection transmission can achieve better performance. For instance, by contrast with the traditional DAS, the BCQ based RAU selection transmission can improve the error rate performance by nearly one order of magnitude. This is due to the fact that the RAU selection transmission can greatly reduce the number of the interfering signals (from 36 interfering signals to 6 interfering signals). It is also noted that the traditional DAS outperforms the MPL based selection transmission at some positions (from $d = 0.25$ to $d = 0.4$). This may be because at these positions, the channel gain contributed from the macro-diversity in the traditional DAS suppresses the gain of the reduction of the interfering signals. Furthermore, the BCQ based selection transmission outperforms the MPL based selection transmission, but their performance gradually tends to be coincident at the cell edge area.

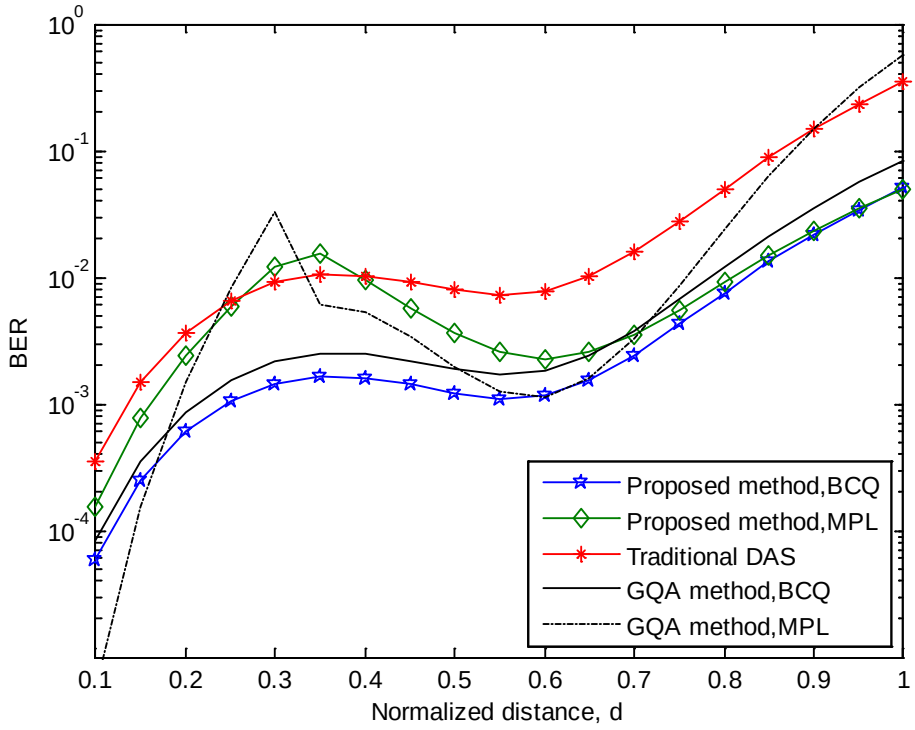

Fig. 4. The error rate with different transmission schemes versus normalized distance

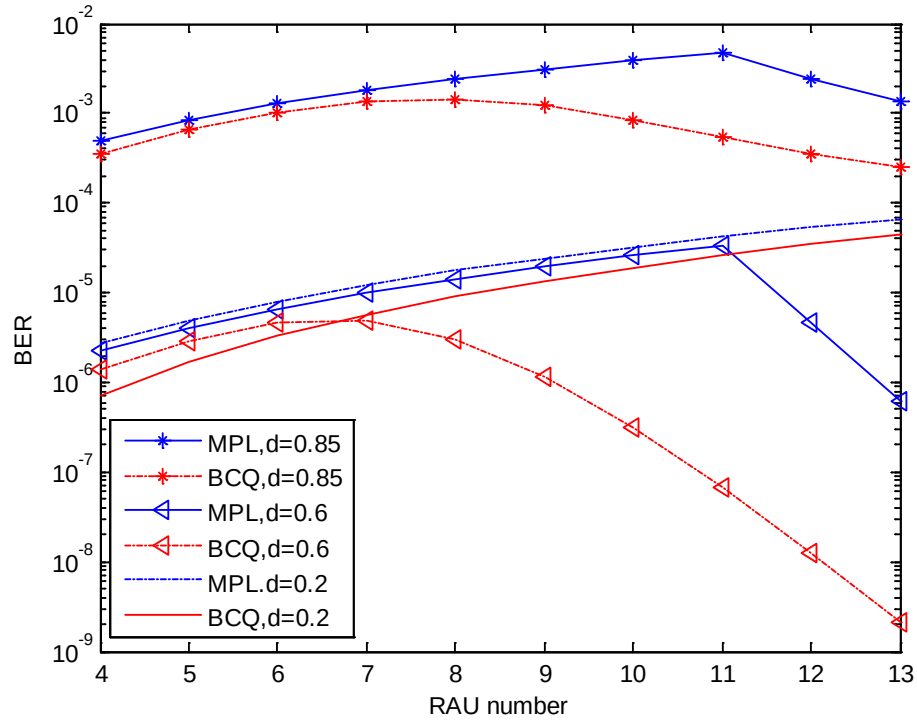

Fig. 5. The error rate versus the number of RAUs in a cell

Since the circularly distributed DAS has flexible infrastructures, the theoretical expressions can efficiently predict the number of the RAUs needed according to the communication requirement, as shown in **Fig. 5**. We select $d = 0.2, 0.6, 0.85$ to represent the cell center area, the improved point, and the cell edge area, respectively. The channel fading severities are set as $m_o^{(0)} = 3$ and $m_I = 2$. As can be seen from **Fig. 5**, the error rate performance improves as the number of RAUs increases when the UE is located at the cell center area. On the contrary, with more RAUs deployed, the error rate performance for the UEs at the cell edge area gets better first and then turns worse after reaching a peak point. For instance, the worst error rate performance for the UEs at cell edge area and improved area based on the MPL and the BCQ selection schemes can be achieved when the numbers of RAUs in a cell are 11 and 7, respectively. This explains the fact that the average distance between the UE and the selected RAU is reduced as the number of RAUs increases, leading to th performance improvement. However, the transmit power of a RAU is decreased if more RAUs are deployed, which degrades the system performance. Thus, the number of RAUs deployed in a cell can be determined if both the performance requirement and the cost are considered.

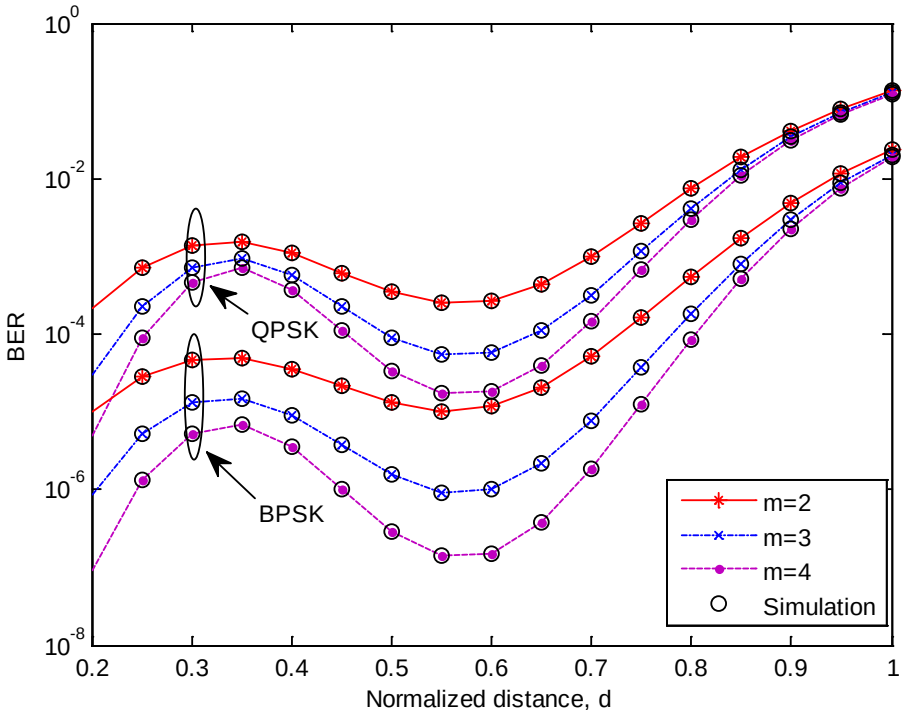

Fig. 6. The error rate of QPSK and BPSK modulation signals based on the BCQ

Fig. 6 depicts the error rate performance of QPSK and BPSK modulation signals with various fading severities when the number of RAUs in a cell is set to be 8. Without loss of generality, we assume all the signals experience the same fading channels ($m_o^{(0)} = m_I = m$). Observe that, the error rate performance improves as the fading becomes more severe, i.e., from $m = 2$ to $m = 4$. Both the BER curves of BPSK modulation signals and QPSK modulation signals have the similar variation tendency as the distance between the UE and the cell center changes. However, BPSK modulation signals have better error rate performance

than QPSK modulation signals. This is because the expected QPSK signal is deteriorated by the CCI from the in-phase and the quadrature channels simultaneously.

5. Conclusion

In this work, we studied the error rate performance of downlink DAS with multicell scenario over Nakagami-*m* fading channels, where arbitrary number of RAUs are deployed in a circular pattern. To alleviate the negative effect of the CCI on the system performance, we used two RAU selection schemes based on the BCQ and the MPL, respectively. Since the in-phase and the quadrature components of the CCI is correlated over Nakagami-m fading channels, a dual-channel receiver has been adopted for the signal detection. Unlike the existing approach in which the desired signal and the CCI are assumed to be a Gaussian noise with fixed variance, we have treated the CCI as the random variable. In addition, the dependency between the in-phase and the quadrature components of the CCI has been considered. For the special case of Rayleigh fading, closed-form error rate expressions have been derived when the dependency between the two components of the CCI could be ignored. Numerical results have validated the correctness of our theoretical analysis by considering the dependency between the in-phase and the quadrature components of the CCI. We also have shown that the RAU selection transmission had performance advantages over the total RAUs transmission. Moreover, QPSK modulation signals have worse error rate performance than BPSK modulation signals at the expense of better bandwidth efficiency.

References

[1] X. Ge, R. Zi, H. Wang, J. Zhang and M. Jo, "Multi-user massive MIMO communication systems based on irregular antenna arrays," *IEEE Transactions on Wireless Communications*, April 2016. Article (CrossRef Link)

[2] Y. Li, G. Zhu, H. Chen, M. Jo and Y. Liu, "SLNR-based user scheduling in multi-cell networks: From multi-antenna to large-scale antenna system," *KSII Transactions on Internet and Information Systems*, vol.8, no.3, pp.945-964, March 2014. Article (CrossRef Link)

[3] H. Kim, S. Lee, C. Song, K. Lee and I. Lee, "Optimal power allocation scheme for energy efficiency maximization in distributed antenna systems," *IEEE Transactions on Communications*, vol.63, no.2, pp.431-440, September 2015. Article (CrossRef Link)

[4] A. Yang, Y. Jing, C. Xing, Z. Fei and J. Kuang, "Performance analysis and location optimization for massive MIMO systems with circularly distributed antennas," *IEEE Transactions on Wireless Communications*, vol. 14, no.10, pp.5659-5671, October 2015. Article (CrossRef Link)

[5] H. Kim, E. Park, H. Park and I. Lee, "Beamforming and power allocation designs for energy efficiency maximization in MISO distributed antenna systems," *IEEE Communications letters*, vol.17, no.11, pp.2100-2103, November 2013. Article (CrossRef Link)

[6] J. Wu, J. Liu, W. Li and X. You, "Low-complexity power allocation for energy efficiency maximization in DAS," *IEEE Communications letters*, vol.19, no.6, pp.925-928, June 2015. Article (CrossRef Link)

[7] J. Wang, L. Dai, "Downlink rate analysis for virtual-cell based large-scale distributed antenna systems," *IEEE Transactions on Wireless Communications*, vol.15, no.3, pp.1998-2011, March 2016. Article (CrossRef Link)

[8] Y. Lin and W. Yu, "Downlink spectral efficiency of distributed antenna systems under a stochastic model," *IEEE Transactions on Wireless Communications*, vol.13, no.12, pp.6891-6902, December 2014. Article (CrossRef Link)

[9] W. Choi and I. G. Andrews, "Downlink performance and capacity of distributed antenna systems in a multicell environment," *IEEE Transactions on Wireless Communications*, vol. 6, no.1, pp. 69-73, February, 2007. Article (CrossRef Link)
[10] H. Zhu, "Performance comparison between distributed antenna and microcellular systems," *IEEE Journal on Selected Areas in Communications*, vol.29, no.6, pp.1151-1163, June 2011. Article (CrossRef Link)
[11] H. Zhu, "On frequency reuse in cooperative distributed antenna systems," *IEEE Communications Magazine*, vol.50, no.4, pp.85-89, April 2012. Article (CrossRef Link)
[12] J. Park, E. Song and W. Sung, "Capacity analysis for distributed antenna systems using cooperative transmission schemes in fading channels," *IEEE Transactions on Wireless Communications*, vol.8, no.2, pp.586-592, February 2009. Article (CrossRef Link)
[13] J. Li, J. Yan, L. Zhao and Q. Dong, "Antenna selection and transmit beamforming optimization with partial channel state information in distributed antenna systems," *IET Communications*, vol.8, no.13, pp.2272-2280, September 2014. Article (CrossRef Link)
[14] H. Li, G. Koudouridis and J. Zhang, "Antenna selection schemes for energy efficiency in distributed antenna systems," in *Proc. of IEEE Int. Conf. on Communications*, pp.5619-5623, June 10-15, 2012. Article (CrossRef Link)
[15] Y. Liu, J. Liu, W. Guo, L. Zheng and P. Chen, "A single transmission selection scheme for downlink distributed antenna system in multicell environment," *International Journal of Communication Systems*, vol.27, no.12, pp.3748-3758, May 2013. Article (CrossRef Link)
[16] Y. Liu, P. Cheng, H. Ouyang, "Bit error rate of SSTS for downlink distributed antenna systems in multicell environment," *Wireless Personal Communications*, vol.3, no.81, pp.1063–1078, November 2015. Article (CrossRef Link)
[17] X. Pang, A. Caballero, A. Dogadaev, et al., "25 Gbit/s QPSK hybrid fiber-wireless transmission in the W-Band (75–110 GHz) with remote antenna unit for in-building wireless networks," *IEEE Photonics Journal*, vol.4, no.3, pp.691-698, June 2012. Article (CrossRef Link)
[18] Y. Yao and A. U. H. Sheikh, "Investigation into cochannel interference in microcellular mobile radio systems," *IEEE Transactions on Vehicular Technology*, vol.41, no.2, pp.114-123, May 1992. Article (CrossRef Link)
[19] J. Cheng, N. C. Beaulieu and D. Zhang, "Precise BER analysis of dual-channel reception of QPSK in Nakagami fading and cochannel interference," *IEEE Communications letters*, vol.9, no.4, pp.316-318, April 2005. Article (CrossRef Link)
[20] I. S. Gradshteyn and I. M. Ryzhik, *Table of Integrals, Series and Products*, 7th Edition, Academic Press, New York, 2003.
[21] M. Abramowitz and I. A. Stegun, *Handbook of Mathematical Functions with Formulas, Graphs, and Mathematical Tables*, 10th Edition, Dover Publications, New York, 1972.

Qing Wang received the M.S. degree in Electronic Engineering from the University of Electronic Science and Technology of China (UESTC), China, in 2008. He is currently a Ph.D candidate in the School of Information Science and Engineering at Shandong University (SDU), China. From September 2013 to September 2014, he was a visiting researcher in the School of Engineering, the University of British Columbia (UBC), Canada. His research interest includes distributed antenna systems, massive MIMO, and energy harvesting for wireless communications

Ju Liu received his B.S. and M.S. degrees both in Electronic Engineering from Shandong University (SDU), Jinan, China, in 1986 and 1989, respectively and his Ph.D degree in Signal Processing from Southeast University (SEU), Nanjing, China, in 2000. Since July 1989, he has been with the Department of Electronic Engineering of SDU. At present he is a professor with the School of Information Science and Engineering at SDU. His current research interests include space-time processing in wireless communication, blind signal separation, and multimedia communications.

Lina Zheng received her B.S. degree in Communication Engineering from Shandong University (SDU) in 2001 and M.S. and Ph.D degrees in Communication and Information System from Shandong University in 2004 and 2011, respectively. Since July 2004, she has been with the School of Information Science and Engineering at SDU. Her research interests include cross-layer design, cooperative communications, and routing algorithm in wireless ad hoc networks.

Hailiang Xiong received the B.Sc. and Ph.D. degrees in communication and information systems from XiDian University, Xi'an, China, in 2005 and 2011, respectively. From 2009 to 2011, he was a visiting scholar at University of Sheffield (UK) and University of Bedfordshire (UK). Currently, he is a lecturer at the school of Information Science and Engineering, Shangdong University. His research interests include digital communication, ultra wideband radio, navigation and positioning.